Freshwater Forcing of Abrupt Climate Change During the Last Glaciation

Peter U. Clark *et al.*

Science **293**, 283 (2001);
DOI: 10.1126/science.1062517

10. M. R. Palmer, *Geology* **19**, 215 (1991).
11. T. Ishikawa, E. Nakamura, *Nature* **370**, 205 (1994).
12. M. Chaussidon, A. Jambon, *Earth Planet. Sci. Lett.* **121**, 277 (1994).
13. T. Ishikawa, F. Tera, *Earth Planet. Sci. Lett.* **152**, 123 (1997).
14. M. Chaussidon, G. Libourel, *Geochim. Cosmochim. Acta* **57**, 5053 (1993).
15. E. Stolper, S. Newman, *Earth Planet. Sci. Lett.* **121**, 293 (1994).
16. M. Chaussidon, B. Marty, *Science* **269**, 383 (1995).
17. A. E. Moran, V. B. Sisson, W. P. Leeman, *Earth Planet. Sci. Lett.* **111**, 331 (1992).
18. G. E. Bebout, J. G. Ryan, W. P. Leeman, *Geochim. Cosmochim. Acta* **57**, 2227 (1993).
19. S. M. Peacock, R. L. Hervig, *Chem. Geol.* **160**, 281 (1999).
20. T. Nakano, E. Nakamura, *Phys. Earth Planet. Inter.*, in press.
21. C.-F. You, A. J. Spivack, J. M. Gieskes, J. B. Martin, M. L. Davisson, *Mar. Geol.* **129**, 351 (1996).
22. N. Shimizu, T. L. Grove, *Abstract Volume of AGU Fall Meeting* (American Geophysical Union, Washington, DC, 1998).
23. M. J. Defant, M. S. Drummond, *Nature* **347**, 662 (1990).
24. W. P. Leeman, D. R. Hildreth, Z. Palacz, N. Rogers, *J. Geophys. Res.* **95**, 19561 (1990).
25. M. B. Baker, T. L. Grove, R. Price, *Contrib. Mineral. Petrol.* **118**, 111 (1994).
26. H. J. Smith, W. P. Leeman, J. Davidson, A. J. Spivack, *Earth Planet. Sci. Lett.* **146**, 303 (1997).
27. A. J. Spivack, J. M. Edmond, *Geochim. Cosmochim. Acta* **51**, 1033 (1987).
28. M. R. Palmer, A. J. Spivack, J. M. Edmond, *Geochim. Cosmochim. Acta* **51**, 2319 (1987).
29. We thank M. Chaussidon, P. B. Kelemen, and K. T. Koga for fruitful discussions, and the other regular Woods Hole geology and geophysics seminar participants for their constructive comments. Supported by Programme Lavoisier, France, and by a J. Steward Johnson scholarship from Woods Hole (E.F.R.).

7 February 2001; accepted 12 June 2001

Freshwater Forcing of Abrupt Climate Change During the Last Glaciation

Peter U. Clark,[1]* Shawn J. Marshall,[2] Garry K. C. Clarke,[3] Steven W. Hostetler,[4] Joseph M. Licciardi,[1]† James T. Teller[5]

Large millennial-scale fluctuations of the southern margin of the North American Laurentide Ice Sheet occurred during the last deglaciation, when the margin was located between about 43° and 49°N. Fluctuations of the ice margin triggered episodic increases in the flux of freshwater to the North Atlantic by rerouting continental runoff from the Mississippi River drainage to the Hudson or St. Lawrence Rivers. We found that periods of increased freshwater flow to the North Atlantic occurred at the same time as reductions in the formation of North Atlantic Deep Water, thus providing a mechanism for observed climate variability that may be generally characteristic of times of intermediate global ice volume.

A leading hypothesis about the origin of the large and abrupt fluctuations in high-latitude climate on millennial time scales invokes changes in the rate of formation of North Atlantic Deep Water (NADW) and their attendant effect on oceanic heat transport (*1*, *2*). Numerous modeling studies demonstrate that the Atlantic thermohaline circulation (THC) is sensitive to the freshwater budget at the sites of deepwater formation (*3*–*5*): Increased freshwater flux to the North Atlantic decreases the formation of deep water, thereby reducing meridional heat transport, which causes cooling of the high latitudes. During glaciations, the circum–North Atlantic ice sheets would have been a ready source of fresh water, but in most cases the causes of increased freshwater flux from these ice sheets to the North Atlantic and their exact relationship to abrupt climate change are unknown. The best-documented case of such freshwater forcing occurred during the Younger Dryas cold interval, when continental runoff that was rerouted from the Mississippi River to the St. Lawrence River at 11,000 ^{14}C years before the present (yr B.P.) [13,000 calendar yr B.P. (cal yr B.P.)] reduced NADW formation (*6*–*9*). This mechanism for large-scale cooling has been regarded as unique to the Younger Dryas, however, and alternative mechanisms have been proposed to explain other millennial-scale climate fluctuations (*10*). Our new reconstructions of North American runoff (*11*, *12*) suggest that the freshwater rerouting that caused the Younger Dryas was, in fact, one of a number of similar events that occurred when the southern margin of the Laurentide Ice Sheet (LIS) was located in the Great Lakes region (Fig. 1). Here, we compare our time series of North American runoff during the last deglaciation to high-resolution records of North Atlantic climate and conclude that these other rerouting events caused abrupt climate change in the North Atlantic region similar to that of the Younger Dryas.

Proxy records of climate and ocean circulation since the last glacial maximum (LGM) indicate that initial warming in the North Atlantic region was accompanied by an increase in the rate of THC (Fig. 2). Assuming that the detrended record of atmospheric radiocarbon (Δ^{14}C) is primarily a signal of ocean circulation (*13*), the post-LGM decrease in Δ^{14}C suggests that THC increased to essentially interglacial levels by 19,000 cal yr B.P. (19.0 cal kyr B.P.) (Fig. 2B). The Greenland oxygen isotope (δ^{18}O record), on the other hand, indicates that air temperatures remained relatively cold, which suggests that low atmospheric greenhouse gas concentrations and large ice sheets partially attenuated ocean-induced warming of the North Atlantic region. In addition, convection in the North Atlantic basin may have been restricted to intermediate depths, which allowed substantial sequestering of atmospheric ^{14}C while contributing less heat than would have been released from deepwater formation (*13*).

Our reconstruction of rerouting events suggests that these initial deglacial warming trends were subsequently reversed by three sequential periods of increased freshwater flow to the North Atlantic originating from two rerouting events through the Hudson River (labeled R7 and R8 in Fig. 2F) that bracket increased iceberg discharge, culminating in Heinrich event 1 (Fig. 2E). During this Oldest Dryas cold event, proxies of ocean circulation identify a long-term decrease in the rate of THC that was episodically interrupted by large variations in the rate, depth, or location of deepwater formation (Fig. 2, B and C). The climate of the North Atlantic region remained cold during the Oldest Dryas (Fig. 2A), suggesting that despite apparent variability in deepwater formation, the net meridional heat transport into the North Atlantic basin remained reduced.

The abrupt warming of the Bølling at 12.8 ^{14}C kyr B.P. (14.6 cal kyr B.P.) coincides with the end of the second rerouting event through the Hudson River (Fig. 2). Proxies of ocean circulation imply that THC also increased to interglacial levels similar to those preceding the Oldest Dryas (Fig. 2B). In contrast to pre–Oldest Dryas conditions, however, the invigorated THC at the start of the Bølling was accompanied by an increase in

[1]Department of Geosciences, Oregon State University, Corvallis, OR 97333, USA. [2]Department of Geography, University of Calgary, Calgary, Alberta T2N 1N4, Canada. [3]Department of Earth and Ocean Sciences, University of British Columbia, Vancouver, British Columbia V6T 1Z4, Canada. [4]U.S. Geological Survey, Department of Geosciences, Oregon State University, Corvallis, OR 97331, USA. [5]Department of Geological Sciences, University of Manitoba, Winnipeg, Manitoba R3T 2N2, Canada.

*To whom correspondence should be addressed. E-mail: clarkp@ucs.orst.edu

†Present address: Department of Marine Chemistry and Geochemistry, Woods Hole Oceanographic Institution, Woods Hole, MA 02543, USA.

temperature to essentially interglacial values (*14*), reflecting the effects of smaller ice sheets, higher atmospheric greenhouse gas concentrations, and the establishment of vigorous NADW formation.

The relations between changes in the fluxes of fresh water, THC, and climate indicate that the prolonged freshwater forcing during the Oldest Dryas delayed the transition from a glacial to an interglacial climate in the North Atlantic region by suppressing formation of NADW. Moreover, although our estimates suggest that the total flux of fresh water from North America to the Atlantic basin remained substantially higher than the modern flux throughout the deglaciation (*11*), our results support modeling studies (*5*, *7*–*9*) in showing that the most important factor in causing changes in the Atlantic THC is the location of freshwater injection: Increased freshwater flow through eastern outlets suppresses THC, whereas the diversion of fresh water to the Mississippi favors more vigorous THC. Further support for this hypothesis is drawn from the relations between subsequent rerouting events and abrupt climate change that we describe next.

The three centennial-scale climate fluctuations that occurred during the Bølling-Allerød warm interval may be linked to three rerouting events (R4, R5, and R6) that were controlled by the position of the southern margin of the LIS (Fig. 2). Each of these events is associated with changes of 20 to 25 per mil (‰) in $\Delta^{14}C$ (*15*), suggesting a reduction in THC.

The onset of the Younger Dryas cold interval at 11.0 ^{14}C kyr B.P. (13.0 cal kyr B.P.) coincided with the diversion of drainage from the Mississippi River to the St. Lawrence River as the ice margin retreated out of the Lake Superior basin (*6*). Abrupt drainage of Lake Agassiz waters (9.5×10^{12} m^3 of water) during the initial stages of this diversion (*16*) may have sensitized the North Atlantic to the increased flux through the St. Lawrence River associated with the rerouting of continental drainage (R3), which nearly doubled the amount of fresh water flowing through the St. Lawrence River (Fig. 2) (*17*). Additional increases in fresh water flowing to the North Atlantic during the Younger Dryas were supplied by icebergs released through the Hudson Strait during Heinrich event 0 (*18*) and from rapid draining of the Baltic Ice Lake along the southern margin of the Scandinavian Ice Sheet (*19*, *20*). Paleocirculation proxies (Fig. 2, B and C) suggest a significant reduction in NADW formation during the Younger Dryas (*21*). The readvance of the ice margin across the eastern outlet of Lake Agassiz at ~10.0 ^{14}C kyr B.P. (11.4 cal kyr B.P.) caused an abrupt decrease in the freshwater flux through the St. Lawrence River by rerouting drainage to other outlets, marking the end of the Younger Dryas (*22*).

The brief (~150-year) Preboreal oscillation occurred ~300 years after the end of the Younger Dryas (Fig. 2). A second draining of the Baltic Ice Lake (*19*, *20*) may have induced the short-lived cooling.

The next substantial increase in the flux of North American fresh water to the North Atlantic (R2) again occurred through the St. Lawrence River, starting ~9.1 ^{14}C kyr B.P. (~10.3 cal kyr B.P.) and continuing until ~7.7 ^{14}C kyr B.P. (~8.4 cal kyr B.P.) (Fig. 2). Like the preceding Younger Dryas age rerouting event through the St. Lawrence River, this event began with the abrupt release of a large volume of water (2.5 to 7×10^{12} m^3) stored in proglacial Lake Agassiz (*16*), followed by a lesser, but sustained, increase in flux of fresh water that was still substantially higher than that preceding the event. Unlike the Younger Dryas, however, the primary climatic response to this rerouting event appears to be to the initial draining of Lake Agassiz, as indicated by proxy records from the North Atlantic region that identify a reduction in the formation of NADW (Fig. 2C) and a cooling at this time (*19*, *23*). Several other proxies record substantial climatic variability in the North Atlantic region during the subsequent period of increased flux of fresh water (*24*, *25*), possibly in response to a weakened THC (*26*). The lack of a sustained climatic response to the sustained freshwater forcing during this period (as compared to the Younger Dryas) may reflect a more vigorous interglacial THC and the lack of additional freshwater sources, such as iceberg discharge during a Heinrich event.

The final substantive rerouting event of the last deglaciation (R1) occurred when the center of the LIS over Hudson Bay collapsed at ~7.7 ^{14}C kyr B.P. (~8.4 cal kyr B.P.) (Fig. 2), allowing the remaining large proglacial lakes to release on the order of 2×10^{14} m^3 of lake water in less than 100 years through the Hudson Strait (*27*). We find that the collapse of the LIS also led to the capture of a large portion of the interior continental drainage (3.4×10^6 km^2) by the Hudson Strait (*11*), resulting in a large increase in freshwater flux through this outlet that was sustained until the final melting of the

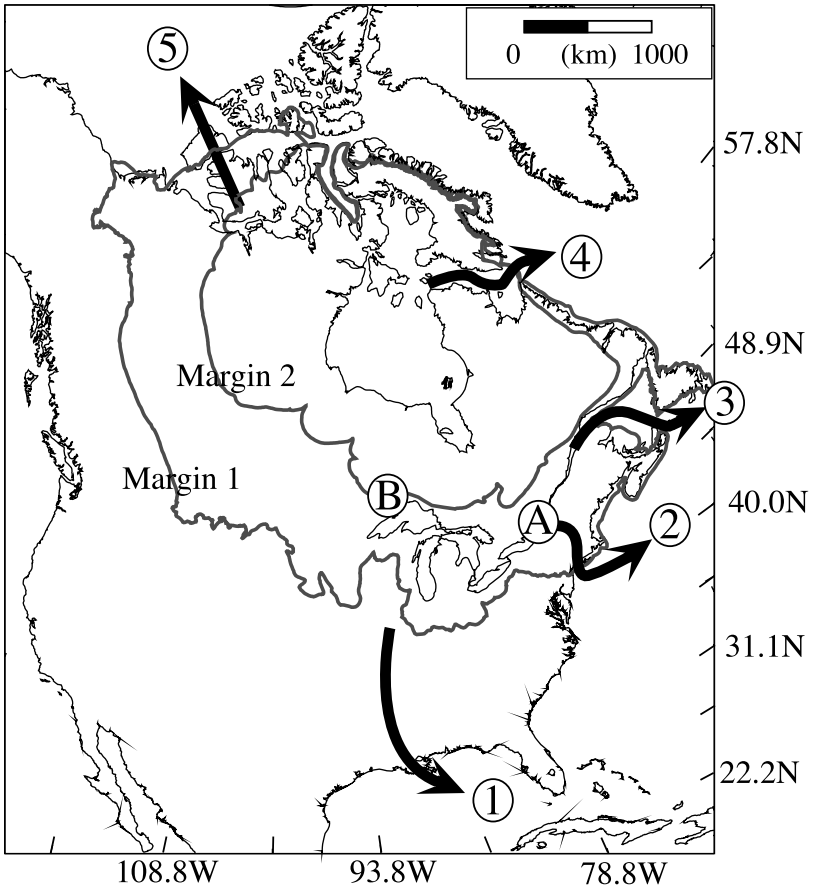

Fig. 1. Map of North America showing the margin of the LIS at its last maximum extent at ~21 cal kyr B.P. (line labeled "margin 1") and at a recessional position at ~13 cal kyr B.P. (line labeled "margin 2") (*34*). The numbers identify five routes of continental runoff: 1, Mississippi River; 2, Hudson River; 3, St. Lawrence River; 4, Hudson Strait; 5, Arctic Ocean. Key locations where routing changes occurred are identified as (A) the eastern outlet from the southern Great Lakes region to the Hudson River and (B) the eastern outlet from the Lake Agassiz basin to the St. Lawrence River. Fluctuations of the southern LIS margin cause routing changes between the two eastern outlets (the Hudson and St. Lawrence Rivers) and the southern outlet (the Mississippi River) only when the ice sheet is of intermediate size.

ice sheet at ~7.0 ^{14}C kyr B.P. (7.8 cal kyr B.P.) (Fig. 2). Collapse of the ice sheet center thus resulted in a two-stage sequence of freshwater forcing similar to that of the two preceding rerouting events.

The final sequence of rerouting related to collapse of the LIS is associated with a ~400-year-long cold event centered on 8.2 cal kyr B.P. that is well expressed in a number of marine and terrestrial records in the circum–North Atlantic region (*28*), although the event has yet to be associated with any deep ocean response (Fig. 2). The absence of a response in Δ^{14}C may indicate that North Atlantic intermediate or deepwater formation had increased at a site away from the point of discharge.

Based on the routing history associated with the LIS during the last deglaciation, we conclude that changes in routing occurred most frequently along the southern ice margin when it was located in the Great Lakes region of central North America (*11*). Results from a coupled ice sheet–surface hydrology model display a similar behavior (*12*). Between ~60 and 22 kyr ago, the model simulates greatest variability in the computed freshwater fluxes to the North Atlantic through the Mississippi and St. Lawrence Rivers, with the same fundamental behavior of ice margin advance and retreat that gives rise to the antiphased routing structure recorded in the geological record of the last deglaciation. While the modeled southern margin of the LIS remained at its LGM position from ~22 to 17 kyr ago, most freshwater was diverted southward to the Mississippi River, and millennial-scale changes in rerouting events did not resume until the ice margin retreated north of this position during deglaciation.

Millennial-scale ice margin fluctuations in the Great Lakes region occurred during longer, orbital-scale (10^4 to 10^5 years), ice margin fluctuations in this region, thus implying two distinct controls of the position of the southern ice margin that operated on different time scales. On the orbital time scale, the ice margin responded to climate changes associated with global boundary conditions, such as insolation, atmospheric greenhouse gas concentrations, and ocean circulation. Internal ice sheet dynamics may have been particularly important during deglaciations. Explaining the millennial-scale fluctuations of the ice margin has been more problematic, but the relation we document here suggests that these fluctuations in the Great Lakes region may have been part of an oscillatory behavior that controlled rerouting events and abrupt changes in North Atlantic sea surface temperatures (SSTs) (Fig. 3). Schematically, retreat of the margin occurred in response to warmer conditions in the North Atlantic region, allowing runoff to be rerouted to the east and out the Hudson River when the margin retreated north of ~43°N (Fig. 1). Increased flux of fresh water through this outlet suppressed NADW formation that caused cooling of the

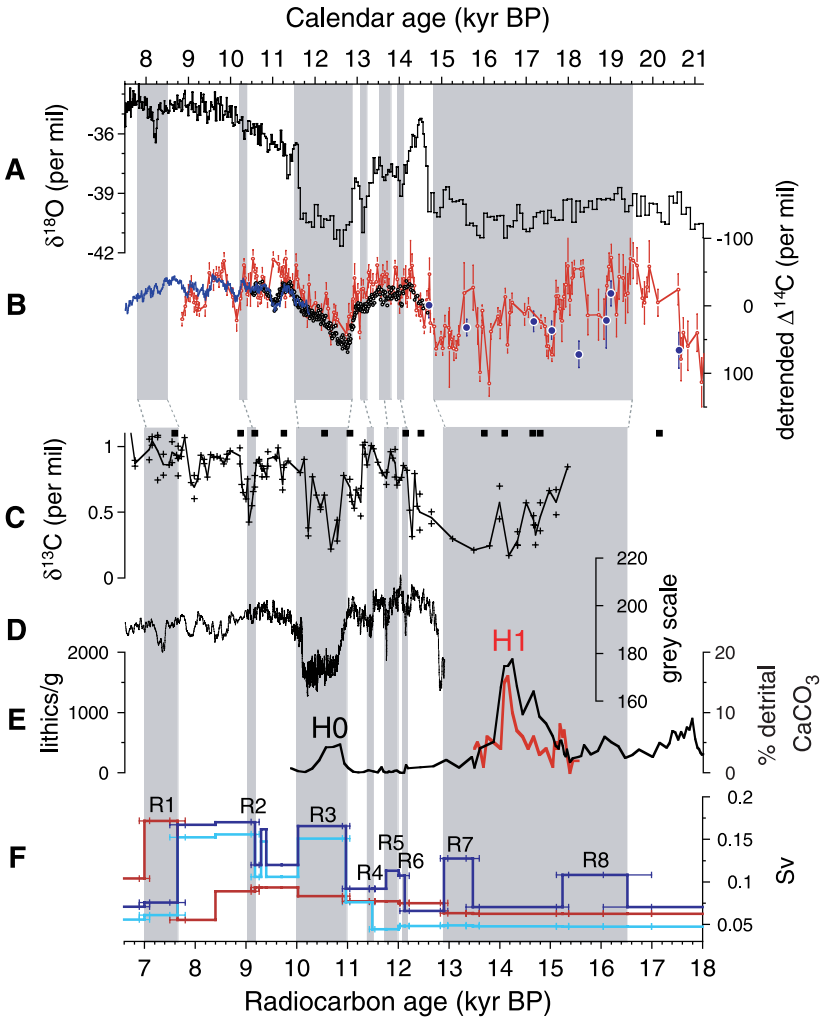

Fig. 2. Records of climate and freshwater fluxes to the North Atlantic between 6.6 ^{14}C kyr B.P. (7.5 cal kyr B.P.) and 18.0 ^{14}C kyr B.P. (21.2 cal kyr B.P.). The time series in (A) and (B) are in calendar years, whereas the time series in (C) through (F) are in radiocarbon years, with the radiocarbon time scale only anchored to the calendar time scale through calibration of the starting and ending radiocarbon ages, using CALIB 4.2 (*38*). The vertical gray bars correspond to times of rerouting events discussed in the text and to Heinrich events 1 and 0 (H1 and H0), identified from records in (E) and (F). Correlation of several radiocarbon-dated events in (F) with the records on a calendar-year time scale is determined by identifying the location of radiocarbon-dated routing events from (F) in the radiocarbon-dated Cariaco basin record (D) and placing them in the same location in the Greenland Ice Sheet Project 2 (GISP2) oxygen isotope record (A), based on the argument that the Cariaco and GISP2 records are in phase (*25*). Correlation of those events either preceding or not present in the Cariaco basin record is done by calibrating the radiocarbon ages using CALIB 4.2. (**A**) The oxygen isotope record from a GISP2 ice core, in per mil (*39*, *40*). (**B**) Changes in atmospheric radiocarbon concentration (Δ^{14}C) (*13*), in per mil, from corals (blue dots) (*41*); varved lake sediments of Lake Suigetsu, Japan (red line) (*42*); the Cariaco basin (black circles) (*15*); and tree rings (green line) (*38*). The four data sets were combined and linearly detrended for the interval from 5 to 25 cal kyr B.P. to derive the plotted record of residual Δ^{14}C. (**C**) Measurements of δ^{13}C from core marine VM29-191 at a water depth of 2370 m (plus signs) (G. Bond, personal communication, 2000); squares across the top are radiocarbon ages (*24*, *43*) that we used to develop the age model of δ^{13}C data. The relatively low resolution of this record precludes identification of centennial-scale events. (**D**) Gray scale data from the Cariaco basin (*25*). A time scale revised from that in (*25*) is available from the World Data Center–A for Paleoclimatology (www.ngdc.noaa.gov/paleo). (**E**) Concentrations of lithic grains per gram of sediment (black curve) and detrital carbonate (red curve) from marine core VM23-081 (*24*). The peak in detrital carbonate at ~14.3 ^{14}C kyr B.P. corresponds to Heinrich event 1 (H1), whereas the peak in lithic grains between ~10.5 and 10.9 ^{14}C kyr B.P. represents Heinrich event 0 (H0). (**F**) Geologically based time series of combined Hudson River and St. Lawrence River runoff (dark blue line), St. Lawrence River runoff (light blue line), and Hudson Strait runoff (red line) in units of Sv (1 Sv = 10^6 m^3 s^{-1}) (*11*). The horizontal error bars represent 1σ uncertainty in the weighted means of radiocarbon ages used to define times of routing changes. Each rerouting event is identified numerically (R1 through R8). The age of the onset of the first routing event (R8 at 16.5 ± 0.5 ^{14}C kyr B.P.) is the least well constrained of all of our events, but stratigraphic evidence clearly demonstrates widespread ice margin retreat and eastward drainage through the Hudson River during this time (*44*).

North Atlantic. Colder conditions allowed the ice margin to readvance and eventually block the eastern outlet, which decreased the outflow of fresh water to the North Atlantic. Subsequently, the rate of NADW formation increased and reestablished warming. Sensitivity tests with a global climate model support this hypothesis, in that cold North Atlantic SSTs cause increased mass balance along the southern LIS margin and warm North Atlantic SSTs cause decreased mass balance (*29*). In addition, ice sheet modeling suggests that the thin and low-sloping ice of the southern LIS that rested on a low-friction substrate facilitated changes in the position of the southern LIS margin by responding rapidly to millennial-scale atmospheric forcing (*30*). In our hypothesized model (Fig. 3), the rerouting events provide the critical mechanism that links the ice margin fluctuations to SST changes.

Regional climate modeling results (*31*) identify an additional oscillatory behavior involving lake–atmosphere–ice sheet interactions that would have occurred when the ice margin was located near the critical eastern outlet at ~49°N (Fig. 1). This lake-effect oscillation may also have induced fluctuations of the ice margin, leading to the diversion of fresh water between the Mississippi and St. Lawrence Rivers.

Our proposed feedback models share important characteristics with the salt-oscillator hypothesis (*10*), which postulates that warm

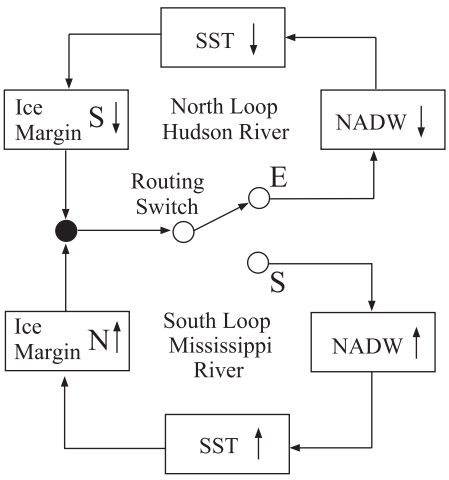

Fig. 3. Schematic representation of oscillatory behavior involving changes in routing to the east (via the Hudson River) and to the south (via the Mississippi River), in NADW, in North Atlantic SSTs, and in the trajectory of the southern LIS margin (southern advance and northern retreat). Routing of fresh water through the Hudson River causes a reduction in NADW formation, thus causing a reduction in SSTs and a subsequent advance of the ice margin. When the ice margin advances across the drainage outlet to the Hudson River, freshwater routing switches to the Mississippi River, resulting in an increase in NADW formation that increases SSTs, thus causing the ice margin to retreat.

North Atlantic SSTs increased the melting rate of (and thus the freshwater flux from) adjacent ice sheet margins, and vice versa. We suggest instead, however, that large changes in freshwater flux to the North Atlantic that induced changes in THC were caused by rerouting of continental runoff associated with a fluctuating ice margin. Model sensitivity tests suggest that warmer SSTs may have induced decreases in net moisture (precipitation minus evaporation), whereas colder SSTs may have induced increases in net moisture, on the order of 0.1 Sv (1 Sv = 10^6 m^3 s^{-1}) over the North Atlantic Ocean (*29*); an additional freshwater forcing of magnitude comparable to that of our reconstructed rerouting events. The increased flux of icebergs (*24*) from marine ice sheet margins that occurred in response to cold events in the North Atlantic would have further amplified these feedbacks.

Finally, our mechanism may explain why the intervals of greatest climate instability have occurred during times of intermediate ice volume (*32*, *33*). Routing changes involving fluctuations of the southern LIS margin only occurred when orbital-scale forcing supported an intermediate-sized ice sheet with a corresponding margin located between 43° and 49°N, the region where the ice margin influenced routing between southern and eastern outlets (Fig. 1). The system could have operated essentially as a free-running oscillator for as long as the ice margin remained in this region, inducing high-amplitude climate variations such as those that occurred during the last deglaciation. An LGM-sized ice sheet routed most drainage to the south, whereas a small or absent LIS that did not block eastern outlets promoted the maintenance of stable eastward drainage pathways, thereby stabilizing the climate of the North Atlantic region.

References and Notes

1. W. S. Broecker, D. M. Peteet, D. Rind, *Nature* **315**, 21 (1985).
2. E. A. Boyle, L. D. Keigwin, *Nature* **330**, 35 (1987).
3. T. F. Stocker, D. G. Wright, *Nature* **351**, 729 (1991).
4. _____, W. S. Broecker, *Paleoceanography* **7**, 529 (1992).
5. S. Rahmstorf, *Nature* **378**, 145 (1995).
6. W. S. Broecker *et al.*, *Nature* **341**, 318 (1989).
7. E. Maier-Reimer, U. Mikolajewicz, in *Oceanography, 1988*, A. Ayala-Castanares, W. Wooster, A. Yanez-Arancibia, Eds. (Universidad Nacional Autonoma de Mexico Press, Mexico City, 1989), pp. 87–100.
8. S. Manabe, R. J. Stouffer, *Paleoceanography* **12**, 321 (1997).
9. A. F. Fanning, A. J. Weaver, *Paleoceanography* **12**, 307 (1997).
10. W. S. Broecker, G. Bond, M. Klas, *Paleoceanography* **5**, 469 (1990).
11. J. M. Licciardi, J. T. Teller, P. U. Clark, in *Mechanisms of Global Climate Change at Millennial Time Scales*, vol. 112, *Geophysical Monograph Series*, P. U. Clark, R. S. Webb, L. D. Keigwin, Eds. (American Geophysical Union, Washington, DC, 1999), pp. 177–201. Licciardi *et al.* reconstructed the history of runoff from North America to the North Atlantic since the LGM 18.0 ^{14}C kyr B.P. (21.2 cal kyr B.P.) from model estimates of melt from the LIS (*34*) and of net moisture changes expressed as precipitation minus evaporation (*35*). The total runoff remained essentially constant throughout deglaciation until the final demise of the LIS at ~7.0 ^{14}C kyr B.P. (7.8 cal kyr B.P.), at which time the flux decreased by ~30% to modern values. The total derived runoff was apportioned among 19 drainage basins and routed to the ocean through five possible outlets (Fig. 1). The estimated runoff from one or more basins is rerouted from one outlet to another when the geologic record indicates that the outlets were opened or closed, largely because of ice margin fluctuations. The timing of rerouting events is established from nearly 150 ^{14}C ages that constrain the age of an ice margin fluctuation and associated opening or closing of a drainage outlet that caused a rerouting event. The timing of a specific rerouting event is determined by using the weighted mean and error of the radiocarbon ages that constrain the age of the event.
12. S. J. Marshall, G. K. C. Clarke, *Quat. Res.* **52**, 300 (1999).
13. M. Stuiver and H. A. Polach [*Radiocarbon* **19**, 355 (1977)] define the concentration of atmospheric radiocarbon (Δ^{14}C) as the per mil deviation from a ^{14}C standard after correction for radioactive decay and fractionation. Δ^{14}C is a function of the production rate of ^{14}C in the upper atmosphere and the exchange rate of CO_2 between the atmosphere, biosphere, and deep ocean. Subtracting changes in Δ^{14}C resulting from long-term changes in production rate isolates changes in the carbon cycle that, on shorter time scales ($\leq 10^3$ years), are largely due to changes in the rate of deepwater formation and solar variability. Changes in the long-term production rate are controlled primarily by changes in the geomagnetic field intensity, which Laj *et al.* [*Philos. Trans. R. Soc. London Ser. A* **358**, 1009 (2000)], among others, show has increased gradually from 25 kyr B.P. to 5 kyr B.P. We have approximated the decrease in atmospheric Δ^{14}C arising from gradually increasing geomagnetic field intensity by subtracting a linear trend from the combined record of Δ^{14}C derived from four data sets over the interval from 5 to 25 kyr B.P. (Fig. 2). Although changes in the rate of THC can be inferred from the detrended record of Δ^{14}C, this signal identifies neither the depth nor the location at which deep water formed.
14. J. P. Severinghaus, E. J. Brook, *Science* **286**, 930 (1999).
15. K. A. Hughen, J. R. Southon, S. J. Lehman, J. T. Overpeck, *Science* **290**, 1951 (2000).
16. D. W. Leverington, J. D. Mann, J. T. Teller, *Quat. Res.* **54** 174 (2000).
17. C. G. Rodrigues and G. Vilks [*Quat. Sci. Rev.* **13**, 923 (1994)] argued that although eastward routing of fresh water to the St. Lawrence River began at ~11.0 ^{14}C kyr B.P., a substantial freshening of the Champlain Sea did not occur until ~10.5 ^{14}C kyr B.P., thus disputing the routing event as the cause of the Younger Dryas. We believe that their salinity records have been compromised, however, by the competing effect of isostatic uplift of the Champlain Sea basin, which would cause salinities to progressively decrease as the basin level rose relative to sea level. de Vernal *et al.* [A. de Vernal, C. Hillaire-Marcel, G. Bilodeau, *Nature* **381**, 774 (1996)] and T. C. Moore *et al.* [*Paleoceanography* **15**, 4 (2000)] have argued that there are no isotopic data to support a large increase in fresh water through the Great Lakes to the St. Lawrence River during the Younger Dryas. We derived a planktonic $\Delta\delta^{18}$O record from the record discussed by de Vernal *et al.* by subtracting the global ice volume component (*36*) from their oxygen isotope data in order to identify anomalies ($\Delta\delta^{18}$O) that reflect some combination of changes in SST and salinity. In doing so, we find a distinct 0.5‰ $\Delta\delta^{18}$O anomaly during the Younger Dryas interval that is consistent with a reduction in salinity. Paleontological data reported by de Vernal *et al.* identify a ~10°C reduction in Younger Dryas SSTs in this region that is equivalent to an additional ~2.5‰ anomaly in δ^{18}O (*37*). The oxygen isotopic record reported by Moore *et al.* only includes the first two centuries of the Younger Dryas interval, with a dating uncertainty of ≥200 years, thus providing little constraint on the oxygen isotopic composition during the Younger Dryas.
18. J. T. Andrews *et al.*, *Paleoceanography* **10**, 943 (1995).

19. S Bjorck *et al.*, *Science* **274**, 1155 (1996).
20. P. Boden, R. G. Fairbanks, J. D. Wright, L. H. Burckle, *Paleoceanography* **12**, 39 (1997).
21. R. Muscheler, J. Beer, G. Wagner, R. Finkel, *Nature* **408**, 567 (2000). Muscheler *et al.* have shown that much of the decrease in atmospheric $\Delta^{14}C$ that occurred after the start of the Younger Dryas (Fig. 2B) resulted from a decrease in the production rate of ^{14}C. The residual $\Delta^{14}C$ record suggests that the rate of deepwater formation remained reduced throughout the Younger Dryas.
22. We attribute the end of the routing event through the St. Lawrence River to the Marquette readvance of the Lake Superior lobe of the LIS across the eastern outlet of Lake Agassiz (*34*). The weighted mean radiocarbon age of this event (10.02 ± 0.02), however, is ~200 years younger than the end of the Younger Dryas in the radiocarbon-dated Cariaco basin record (Fig. 2D), but this age difference may be more apparent than real in that it occurs during a radiocarbon plateau that spans this interval. There is no age difference if we used only the oldest accelerator mass spectrometry radiocarbon age on the Marquette readvance (10.2 ± 0.05) rather than the weighted mean radiocarbon age. Finally, one of us (J. T. Teller, *Quat. Sci. Rev.*, in press) suggested that the eastern outlet may have closed ~200 years before the Marquette readvance by isostatic uplift of the eastern outlet, diverting drainage from the Lake Agassiz basin to St. Lawrence River south to the Mississippi River, but there is currently no age control to constrain the timing of this hypothesis.
23. S. Bjorck *et al.*, in preparation.
24. G. Bond *et al.*, *Science* **278**, 1257 (1997).
25. K. A. Hughen, J. T. Overpeck, L. C. Peterson, S. Trumbore, *Nature* **380**, 51 (1996).
26. E. Tziperman, *Nature* **386**, 592 (1997).
27. D. C. Barber *et al.*, *Nature* **400**, 344 (1999).
28. R. B. Alley *et al.*, *Geology* **25**, 483 (1997).
29. S. W. Hostetler, P. U. Clark, P. J. Bartlein, A. C. Mix, N. J. Pisias, *J. Geophys. Res.* **104**, 3947 (1999).
30. J. W. Jenson, D. R. MacAyeal, P. U. Clark, C. L. Ho, J. C. Vela, *J. Geophys. Res.* **101**, 8717 (1997).
31. S. W. Hostetler, P. J. Bartlein, P. U. Clark, E. E. Small, A. M. Solomon, *Nature* **405**, 334 (2000).
32. J. F. McManus, D. W. Oppo, J. L. Cullen, *Science* **283**, 971 (1999).
33. M. Schultz, W. H. Berger, M. Sarnthein, P. M. Grootes, *Geophys. Res. Lett.* **26**, 3385 (1999).
34. J. M. Licciardi, P. U. Clark, J. W. Jenson, D. R. MacAyeal, *Quat. Sci. Rev.* **17**, 427 (1998).
35. J. Kutzbach *et al.*, *Quat. Sci. Rev.* **17**, 473 (1998).
36. R. G. Fairbanks, *Nature* **342**, 637 (1989).
37. R. Zahn, A. C. Mix, *Paleoceanography* **6**, 1 (1991).
38. M. Stuiver *et al.*, *Radiocarbon* **40**, 1041 (1998).
39. P. M. Grootes, M. Stuiver, J. W. C. White, S. J. Johnsen, J. Jouzel, *Nature* **366**, 552 (1993).
40. D. A. Meese *et al.*, *J. Geophys. Res.* **102**, 26411 (1997).
41. E. Bard, M. Arnold, B. Hamelin, N. Tisnerat-Laborde, G. Cabioch, *Radiocarbon* **40**, 1085 (1998).
42. H. Kitagawa, J. van der Plicht, *Radiocarbon* **42**, 369 (2000).
43. I. M. Lagerklint, J. D. Wright, *Geology* **27**, 1099 (1999).
44. J. C. Ridge, *Geol. Soc. Am. Bull.* **109**, 652 (1997).
45. We thank R. Alley, J. Andrews, E. Brook, A. Mix, D. Pollard, A. Weaver, and anonymous reviewers for comments. Supported by the NSF Earth System History program (P.U.C. and S.J.M.), the Natural Sciences and Engineering Research Council of Canada (G.K.C. and J.T.T.), and the U.S. Geological Survey (S.W.H.).

14 May 2001; accepted 12 June 2001

Developmental Changes Due to Long-Distance Movement of a Homeobox Fusion Transcript in Tomato

Minsung Kim,* Wynnelena Canio,* Sharon Kessler, Neelima Sinha†

Long-distance movement of RNA through the phloem is known to occur, but the functional importance of these transported RNAs has remained unclear. Grafting experiments with a naturally occurring dominant gain-of-function leaf mutation in tomato were used to demonstrate long-distance movement of mutant messenger RNA (mRNA) into wild-type scions. The stock-specific pattern of mRNA expression was graft transmissible, indicating that the mRNA accumulation pattern is inherent to the transcript and not attributable to the promoter. The translocated mRNA caused changes in leaf morphology of the wild-type scions, suggesting that the translocated RNA is functional.

Increased plant size and multicellularity require that plant cells and organs communicate with each other so that the organism can develop as a coordinated whole and adapt to the changing environment. Short-distance communication occurs through plasmodesmata. Regulatory proteins such as KNOTTED-1, DEFICIENS, GLOBOSA, and LEAFY may move from cell to cell in a developmentally significant manner (*1*–*3*). Specific and spatially restricted short-distance mRNA movement establishes the postanterior and dorsal-ventral polarity of the early oocyte in *Drosophila* (*4*, *5*). Long-distance movement of water, plant hormones, minerals, sugars, and amino acids occurs through phloem and xylem. Long-distance movement of nucleic acids was first observed in plant viral infections. Viral movement proteins (MP) facilitate the cell-to-cell movement of viral nucleic acids through plasmodesmata by forming MP–nucleic acid complexes (*6*). Similarly CmPP16, a *Cucurbita maxima* paralog to viral movement protein, carries various mRNA molecules from cell to cell (*7*). Other examples of intercellular mRNA movement include *SUCROSE TRANSPORTER1* (*8*), the small RNAs that mediate cosuppression (*9*), and *CmNACP* (*10*). However, in the absence of a phenotypic effect caused by the translocated RNA, the functional importance of long-distance mRNA movement in regulating morphological development in plants remained unclear.

Tomato normally produces unipinnate compound leaves (Fig. 1A), whereas the dominant mutant *Mouse ears* (*Me*) has up to octapinnate compound leaves (Fig. 1D) (*11*). Compared with wild-type leaflets with pinnate venation and acute lobes (Fig. 1B), *Me* leaflets are rounded and unlobed and have palmate venation at the base of the leaflets (Fig. 1E). This phenotype of the *Me* mutant is caused by a gene fusion between *PYROPHOSPHATE-DEPENDENT PHOSPHOFRUCTOKINASE* (*PFP*), an enzyme in the glycolytic pathway, and *LeT6*, a tomato *KNOTTED-1*–like homeobox (*KNOX*) gene. The *PFP-LeT6* fusion gene includes about 10 kb of native *PFP* upstream sequence, allowing for a high-level expression pattern of the functional homeobox fusion transcript in the *Me* plants, leading to extra orders of leaf compounding (*11*–*13*). Wild-type plants [carrying the semidominant *Xanthophyllic* (*Xa*) mutation causing yellow normal leaves] were grafted onto *Me* plants (Table 1). In 11 out of 13 grafts of *Xa* scions on *Me* stocks (*Xa* heterografts), leaves had higher orders of pinnation than normal (Fig. 1G) and rounded lobes that were reduced in number (Fig. 1H). These leaves resembled those produced on plants carrying the *Me* mutation (Fig. 1E) as

Table 1. Phenotypic changes observed after grafting.

Grafts (scion/stock)	Total number of grafts	Number of plants with altered leaf phenotype after grafting	Number of plants with same leaf phenotype after grafting
Me/Me	5	0	5
Xa/Xa	5	0	5
Me/Xa	11	0	11
Xa/Me	13	11	2

Section of Plant Biology, Division of Biological Sciences, University of California–Davis, 1 Shields Avenue, Davis, CA 95616, USA.

*These authors contributed equally to the work.
†To whom correspondence should be addressed. E-mail: nrsinha@ucdavis.edu